THE
TECHNOLOGICAL
INSTITUTE

AERIAL MEASUREMENTS LABORATORY

NORTHWESTERN UNIVERSITY
EVANSTON, ILLINOIS

THE

TECHNOLOGICAL

INSTITUTE

Contract NOw 62-0749-d

Memo No. 385
Copy No. 15

SOLID STATE ANALOG-TO-DIGITAL CONVERTER

Fourth Quarterly Progress Report

February - March - April 1963

Paul G. Sedlewicz Robert E. Onley

AERIAL

MEASUREMENTS

LABORATORY

NORTHWESTERN UNIVERSITY

Evanston, Illinois

CONTENTS

Section	Title	Page
	Abstract	1
I.	Purpose	2
II.	Discussion.	
	A. Introduction	3
	B. Device Handling	3
III.	Investigation	
	A. Movement of Depletion Region	5
	B. Cutoff Characteristics	21
IV.	Summary and Results	31
V.	Future Work	32

ILLUSTRATIONS

Figure	Title	Page
1.	Diffusion from a Concentration Step.....	6
2.	Acceptor and Donor Distribution of PN Wafer.....	9
3.	Capacitance of Reverse Biased PN Wafer.....	15
4.	Movement of Depletion Layer on Bevel.....	20
5.	Forward and Reverse Characteristics of Metal Probes.....	22
6.	V-I Characteristics of Tungsten Probe on Bevel.....	25
7.	Normalized Probe Current with Increasing Depletion Region.....	26
8.	Normalized Probe Current with Increasing Channel Depth.....	27
9.	Probe Cutoff Characteristics.....	30

Table	Title	Page
I.	Data on Diffusion[6].....	7
II.	Field and Potential Distributions of ERFC Junction.....	13

ABSTRACT

This report presents equations for the movement of the depletion region and for multiple probe cutoff. The movement of the depletion region along the bevel is related to an abrupt junction movement times the amplification angle of the bevel. An empirical equation relating the probe current to the reverse bias of the PN bevel is given for the cutoff characteristics.

I. Purpose

The purpose of this contract is to conduct research and development directed toward determining the feasibility of fabricating a solid-state analog-to-digital converter (or ADC). This research is to be based on the movement of the depletion region of a reverse biased PN crystal of silicon and the detection of this movement.

II. Discussion

A. Introduction

The cutoff characteristics of probes positioned on a beveled PN wafer and the movement of the depletion region are directly related. The interaction of the probe current path (channel) with the depletion region causes the cutoff.

The original investigation[1] of the field and potential distributions of our specific PN wafers was not adequate to develop a theoretical cutoff equation. The movement of the depletion region and the cutoff of the probes is complicated by the formation of the junction, beveling of the wafer, current path, etc. During this period the movement and the cutoff were investigated for these considerations and a theoretical model is presented.

The cutoff of multiple probes can be investigated by using a single probe. This single probe was used to obtain experimental data on cutoff and, in conjunction with theoretical considerations, an equation for the cutoff is presented. The limitations of this equation, as to device configurations and characteristics were considered and will be useful in describing device resolution. The equation can be readily adapted to multiple probes, using basic parameters inherent within the device.

B. Device Handling

Modification of an existing manipulator was carried

---

(1) 1st Quarterly Progress Report, Solid State ADC, NOw 62-0749-d, Aerial Measurements Laboratory, Northwestern University, May-June-July, 1962.

out. This modification consisted of the introduction of a micrometer drive to the vertical movement of the adapted Wilder stage and connection of terminals for the three leads from the wafer and probe. This change permits a more accurate positioning of the probe on the beveled surface.

A dry box was obtained for test. It is a commercial plexiglass box with a circulating system for passing the air through desiccant tubes. The system works adequately and appears to produce a sufficiently dry atmosphere in which to work. Stages and other equipment are presently being modified so that the positioning of multiple probes can be carried out conveniently in the dry box.

III. Investigation

A. Movement of Depletion Region

The electrical properties of a reverse biased PN junction are deduced directly from a solution of Poisson's equation in the space charge region. This equation is analytically integrable for many charge distributions and a solution has been given for a diffused junction of the constant surface concentration type.(2) The type of charge distribution is presented and its application to the one-dimensional solution of Poisson's equation is given. This derivation is then modified to represent the characteristic of the beveled PN junction.

The formation of a P-type region within a single crystal of N-type silicon by a diffusion process is represented by a solution of the diffusion equation.(3)

$$\bar{F} = -D\bar{\nabla}N \qquad (1)$$

The diffusion coefficient D is the factor of proportionality relating the flow density $\bar{F}$ of diffusing atoms to the concentration gradient $\bar{\nabla}N$ of the atoms.

The diffusion equation has been solved by Smits for the constant surface concentration where only the initial conditions have been considered.

---

(2) J. Cohen, Transition Region Properties of Reverse Biased Diffused PN Junction, IRE trans., ED-1 September 1961, pp 362-369.

(3) F.M. Smits, Formation of Junction Structure by Solid State Diffusion, Proc. IRE, Vol. 47, No. 69, June 1958, pp 1049-1061

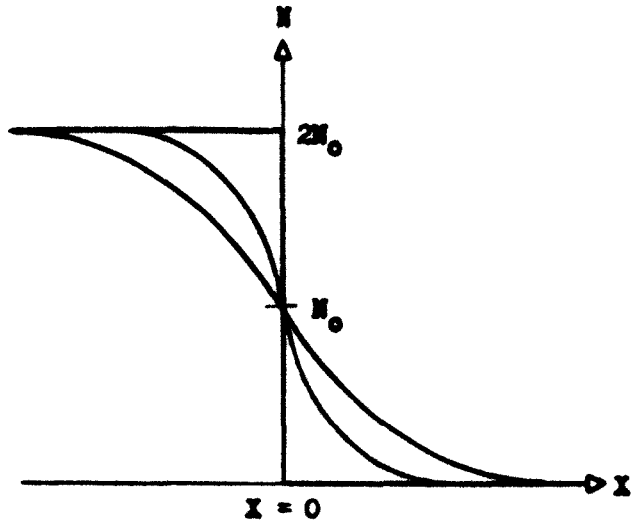

Figure 1. Diffusion from a Concentration Step

The initial conditions can be specified by Figure 1.

$$N = 2N_O \text{ for } X<0$$

$$N = 0 \quad \text{for } X>0$$

where N_O is the surface concentration, constant for all time.

The diffusion from such initial conditions is described by the diffusion equation as:

$$N = N_O \operatorname{erfc} (X/2\sqrt{DT}) \qquad (2)$$

Thus the acceptor impurity distribution will be of the complementary error function type where

N_o is the constant acceptor concentration at the surface (acceptor/cm^3)

X is the distance of diffusion from the surface (cm)

T is the time of diffusion (sec)

D is the diffusion constant of the acceptor (cm^2/sec)

erfc is the complementary error function[4]

The diffusion constant (D), for silicon, has been worked out by Fuller and Ditzenberger.[5]

The PN wafers used were of the constant surface concentration type. Table I lists the diffusion data for these wafers.

Wafer	Substrate	P-type Dopant	Surface Conc. (N_o)	Time	Temp.
B	N type Si 90±10Ω -cm	Boron	10^{20} atoms/cm^3	64 hrs	1260°C
C	N-type Si 100±10Ω -cm	Boron	10^{18} atoms/cm^3	48 hrs	1260°C

Table I. Data on Diffusion[6]

---

(4) Table of the Error Function and its Derivative, U.S.Department of Commerce, National Bureau of Standards Applied with Series 41, issued October 22, 1954.

(5) C. S. Fuller and J. A. Ditzenberger, Diffusion of Donor and Acceptor Elements in Silicon, Journal of Applied Physics, Vol. 27, 1956, pp 544-553.

(6) The wafers were diffused by Hoffman Electronics Co.

Substituting values from Table I into Equation (2) a plot of the acceptor concentration can be obtained. Using the values for wafer B, Equation (2) becomes;

$$N_a(X) = 10^{20} \text{ erfc } (X/21.4 \times 10^{-4})$$

This equation is plotted in Figure 2 where the acceptor concentration as a function of distance from the surface is shown. Also plotted in Figure 2 is the constant donor concentration N_d. The donor concentration was obtained from the standard conductivity equation[7], assuming all donors were ionized. This gives an N_d of 5.3×10 donor atoms per cm^3. The location of the junction is obtained from the plot where

$$N_d - N_a = 0$$

The location, 8.0×10^{-3} cm into the silicon, agrees within experimental error with the location of the junction obtained by the preferential etching technique.[8]

Solution of Poisson's equation for a junction formed by constant surface concentration on a uniform concentration of donors has been derived by Cohen.[9]

---

(7) R. D. Middlebrook, An Introduction to Junction Transistor Theory, John Wiley and Sons, Inc., New York, 1957, Ch. 4

(8) H. Bridges, J. Scoff, J. Shives, Transistor Technology, Vol. 1, 1958, Van Nostrand Co., N.Y.

(9) See Reference (1)

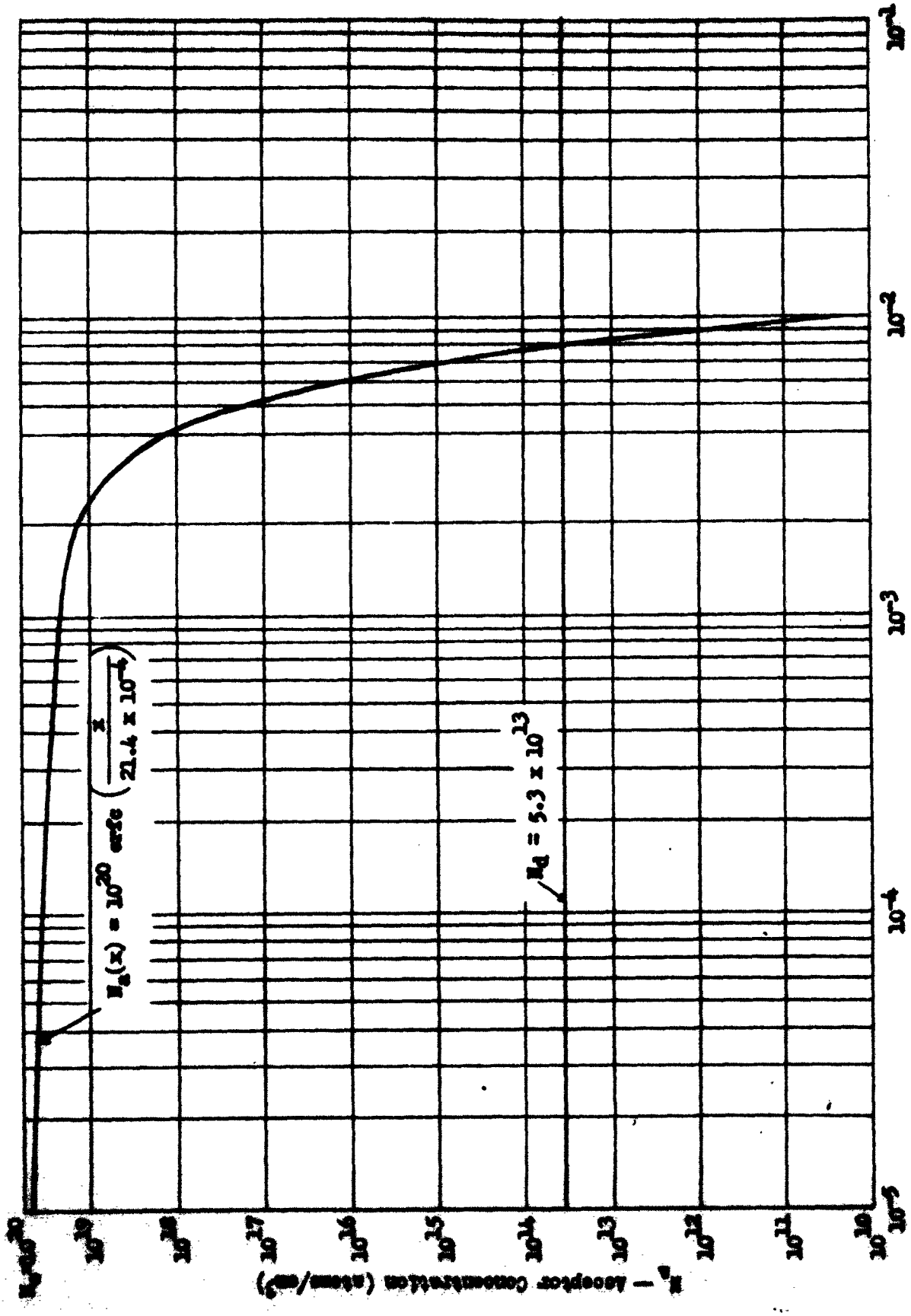

Figure 2. Acceptor and Donor Distribution of PN Wafer

Poisson's Equation in this case is:

$$\frac{d^2V}{dX^2} = \frac{q}{\epsilon}\left(\rho_{(X)}\right) = \frac{q}{\epsilon}\left[N_o \operatorname{erfc}\left(\frac{X}{L}\right) - N_d\right] \qquad (3)$$

where: ϵ is the permittivity of silicon (f/cm)

$L = 2\sqrt{DT}$ is the diffusion length (cm)

Transforming the equation so that it has a single parameter by the following substitution:

$$u = X/L$$

$$W = EV/q\ N_o\ L^2$$

$$N = N_o/N_o$$

Equation (3) reduces to:

$$\frac{d^2W}{du^2} = \operatorname{erfc} u - n \qquad (4)$$

where $n = \operatorname{erfc} u_o$ and u_o is the point of zero net charge. or the junction.

The solutions of Equation (4) are in the form of second integrals of the complementary error function and are difficult to manipulate,[10] but simple approximations can be made.

---

(10) L. Giacoletto, Junction Capacitance and Related Characteristics Using Graded Impurity Semiconductors, IRE, Trans. Vol. ED-4, 1957. pp 207-215.

A graded junction is defined by $(N_d - N_a) = (a)(x-x_o)$ where (a) is a constant. Within the region of the junction a first order Taylor expansion may be used.

$$(N_d - N_a) \approx \left[d(N_d - N_a)/dX_o\right] (X-X_o) \tag{5}$$

Shockley and others[11,12] have shown for a graded junction that

$$D^3 = \frac{L^3 qa}{12\epsilon} \frac{1}{(V_2-V_1)} \tag{6}$$

where

$D = 1/(u_2 - u_1)$ is the normalized width of the depletion region

$V_2 - V_1$ is the potential drop across the junction.

The approximate field and potential distributions can now be obtained using Equations (4), (5), (6). The field distribution becomes:

$$F \approx F_o + 1/2\ (u - u_o)^2\ d\ \text{erfc}\ u_o \tag{7}$$

where $F = \epsilon E/q\ N_o L$, the normalized field

F_o is the normalized field at $u = u_o$

---

(11) W. Shockley, The Theory of PN Junctions in Semiconductor and PN Junction Transistors, Bell Systems Technical Journal, Vol. 28, 1949, pp 435-489.

(12) D. Dewitt and A. Rossoff, Transistor Electronics, McGraw-Hill Company, N.Y., 1957, Ch. 2.

The potential distribution becomes:

$$(W_2 - W_1) \approx d\ \mathrm{erfc}\ u_o/12D^3 \tag{8}$$

where d erfc u is the Gaussian function $2\pi^{-\frac{1}{2}} \exp(-u^2)$, the negative derivative of erfc u.

When the reverse potential across the diffused junction is increased, it leaves the voltage region in which Equation (6) is valid. Since $N_d << N_o$ the junction will enter the region where abrupt junction solution of Poisson's equation is valid.[13] In the abrupt region, the junction behaves very similarly to an infinite-step junction with a background doping of N_d. For such a junction, Shockley[14] has shown that:

$$D^2 = \frac{L^2 \epsilon q N_d}{2\epsilon} \qquad \frac{1}{(V_2 - V_1)} \tag{9}$$

where the potential distribution is given as

$$(W_2 - W_1) = \frac{n}{2} \frac{1}{D^2} \tag{10}$$

and the field distribution is given as

$$F = F_o + n(u - u_o) \tag{11}$$

---

(13) L. B. Valdes, The Physical Theory of Transistors, McGraw-Hill Company, N.Y. 1961, Ch. 10

(14) See Reference (11).

Thus Equations (7), (8), (10) and (11) characterize the potential and field distributions of a diffused PN junction of the constant surface concentration within the linear graded and abrupt regions. Table II gives these equations with the values resubstituted.

	Graded Junction Region	Abrupt Junction Region
Field Distribution	$E = E_o + \frac{qN_o}{2\epsilon L}\left(d\ \text{erfc}\ \frac{X_o}{L}\right)(X-X_o)^2$	$E = E_o + \frac{qN_d}{\epsilon}\ (X-X_o)$
Potential Distribution	$V_2 - V_1 = \frac{qN_o}{12\epsilon L}\left(d\ \text{erfc}\ \frac{X_o}{L}\right)(X_2-X_1)^3$	$V_2 - V_1 = \frac{X_o}{2\epsilon}\ (X_2-X_1)^2$

Table II. Field and Potential Distributions of ERFC Junction

The voltage where the movement of the depletion region changes from Equation (6) to Equation (9) is given by:

$$D\ (\text{graded}) = D\ (\text{abrupt})$$

and transition voltage V_c becomes

$$V_c = \frac{18\ q\ N_o L^2 n^3}{\epsilon(d\ \text{erfc}\ u_o)^2} \qquad (12)$$

Substitution can be made into Equation (12) for the wafers used and tabulated in Table I. Wafer B gives the transition voltage to be

$$V_c \approx 6.4\ (\text{volts})$$

Calculation on wafer C (Table I) gives a transition voltage of

$$V_c \approx 5 \text{ (volts)}$$

Thus, the potential distribution of the wafers over the major portion of the depletion region is of the abrupt junction type and the use of Equation (10) for the abrupt junction distribution is a good approximation.

A capacitance versus reverse bias test was made on wafer C and is shown in Figure 3. The transition from the initial slope (for a linear graded junction movement) to the slope for an abrupt junction movement occurs at approximately 7.5 volts. This shows experimental verification of Equation (12) and further substantiates the use of Equation (10) for the movement of the depletion layer for the wafers.

The field and potential distributions of the constant surface concentration diffusion within the depletion region can be approximated by the abrupt junction equation in the one-dimensional case. This approximation can now be carried over to the beveled PN junction where a two-dimensional field and potential distribution must be considered.

The depletion region of a beveled PN wafer is more complicated than the one-dimensional case. The field and potential distributions within the region of the bevel are now important and are mathematically obtainable from a solution of Poisson's equation in two dimensions. The discussion will be qualitative as to the field and potential distributions, using the laws of space charge neutrality and electrostatic theory.

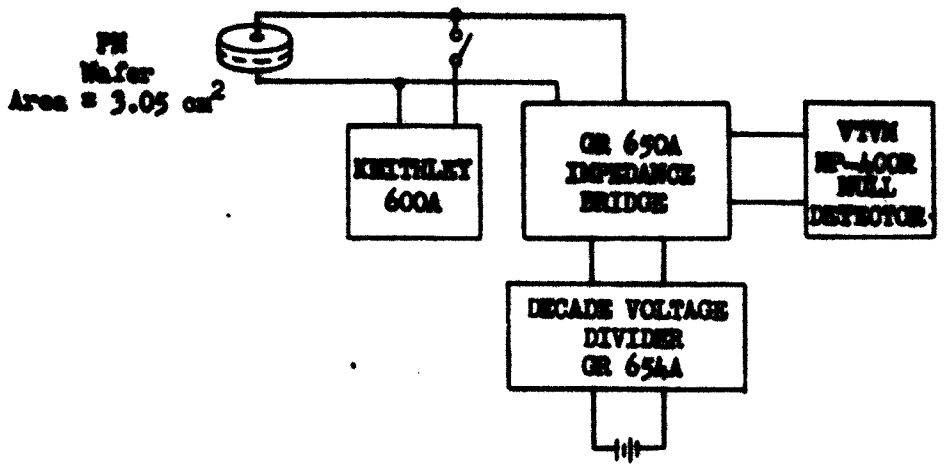

Bias for PN Wafer

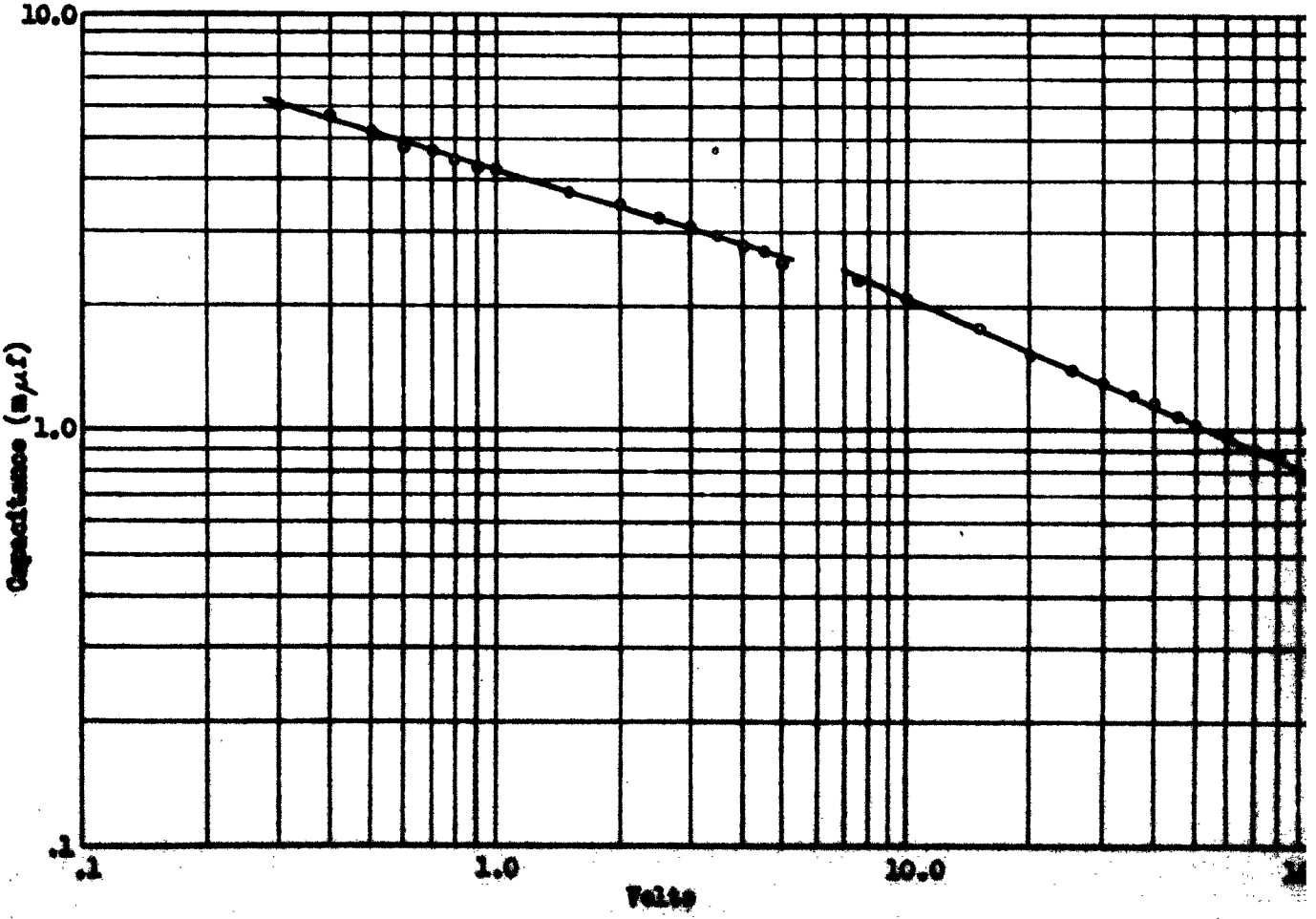

Figure 3. Capacitance of Reverse Biased PN Wafer

The depletion layer is maintained by the fixed ionized donors and ionized acceptors on the N and P sides of the junction respectively. This assumes a negligible number of mobile electrons and holes within the depletion region. Since the donor and acceptor concentrations are fixed throughout the crystal, a fixed field and potential distribution must be established. This can be stated as a space charge neutrality condition within the depletion region:

$$N_a V_p = N_d V_n \tag{13}$$

Equation (13) states that the total negative charge on the P-side of the junction (ionized acceptor) must equal the total positive charge on the N-side of the junction (ionized donor). Beveling across the junction creates a larger volume on the P-side than on the N-side. This requires an increase in the depletion region on the N-side close to the bevel. or a decrease on the P-side, or both. Gauss's Law can be stated so as to relate the normal components of flux density along the bevel between the depletion region and external media.(15)

$$\int_S D_n \, d S = D_{nS} S - D_{n\,air} S = Q \tag{14}$$

This equation states that the normal component of the flux density changes at the boundary by an amount equal to the surface charge density. In the case where the surface charge density is zero,

(15) J. D. Kraus, Electromagnetics, McGraw-Hill Company, New York, 1953, Ch. 1 & 2.

the normal components of D are equal. This requires the equipotential lines to meet the bevel surface perpendicularly, creating an increase in the depletion region on the N-side and a decrease on the P-side.

The ideal case (Q = 0, no surface states, etc.) would indicate an increase in the depletion region at the surface greater than that predicted by the beveling of the PN junction. Since the number of ionized donors at the surface is not zero, and the number of surface states [16,17] can be substantial, the increase will not be as great as predicted in the ideal case. Through this qualitative argument it appears that the width of the depletion region along the bevel will not be increased effectively over that obtained by the amplification angle of the bevel.

This potential and field distribution of the beveled PN wafer can now be related to the one-dimensional solutions discussed previously. It has been shown qualitatively that the decrease in potential (or increase in movement) on the bevel can be related to the ramp angle. This constant can be given as:

$$\theta = \sin \phi \qquad (15)$$

---

(16) H. Statz, G. DeMars, L. Davis, A. Adams, Surface States on Si and Ge Surfaces, Physical Review, Vol. 101, February 1959, pp 1272-1281.

(17) P. Handles, Electrical Properties of the Surface of Semiconductors, The Surface Chemistry of Metals and Semiconductors, John Wiley and Sons, Inc., New York, 1959, pp 54-71

where

ϕ is the angle of the bevel

The potential distribution along the bevel using Equation (10) becomes:

$$(V_2 - V_1)_{bevel} = \theta\,(V_2 - V_1)_{bulk} - \frac{\theta q N_d (X_2 - X_1)^2}{2\epsilon} \qquad (16)$$

where

$(X_2 - X_1)$ is the dimensional movement.

Equation (16) gives the potential distribution along the bevel as a product of the abrupt junction potential distribution times the geometric decrease due to the bevel. Assuming all the potential is dropped across the junction:

$$(V_2 - V_1) = V_R$$

and all the movement is into the N-material (since $\rho_p << \rho_n$);

$$(X_2 - X_1) = X_n$$

where X_n is the movement in the bulk.

Equation (16) can be rewritten as:

$$V_R = \frac{\theta q N_d}{2\epsilon} X_n^2 \qquad (17a)$$

and the width of the depletion region on the bevel is given by

$$X = \frac{1}{\theta}\left[\frac{2\epsilon}{qN_d}\right]^{\frac{1}{2}} V_R^{\frac{1}{2}} \qquad (17b)$$

where X is the movement on the bevel (cm)

Equation (17b) has been verified experimentally by probing for the depletion region with increasing reverse bias. Figure 4 is the experimental curve and theoretical curve (Equation (17b) for a B wafer with a bevel angle of 2° 15'. The values obtained from Table I are:

$$\left[\frac{2\epsilon}{qN_d}\right]^{\frac{1}{2}} = .35 \times 10^{-3} \ (cm^2/volt)^{\frac{1}{2}}$$

$$\frac{1}{\theta} = 25$$

The experimental curve is within experimental error of the theoretical curve throughout the operating voltage range. Thus, the assumptions for the one dimensional solution of the erfc junction and for the bevel region are within experimental tolerance.

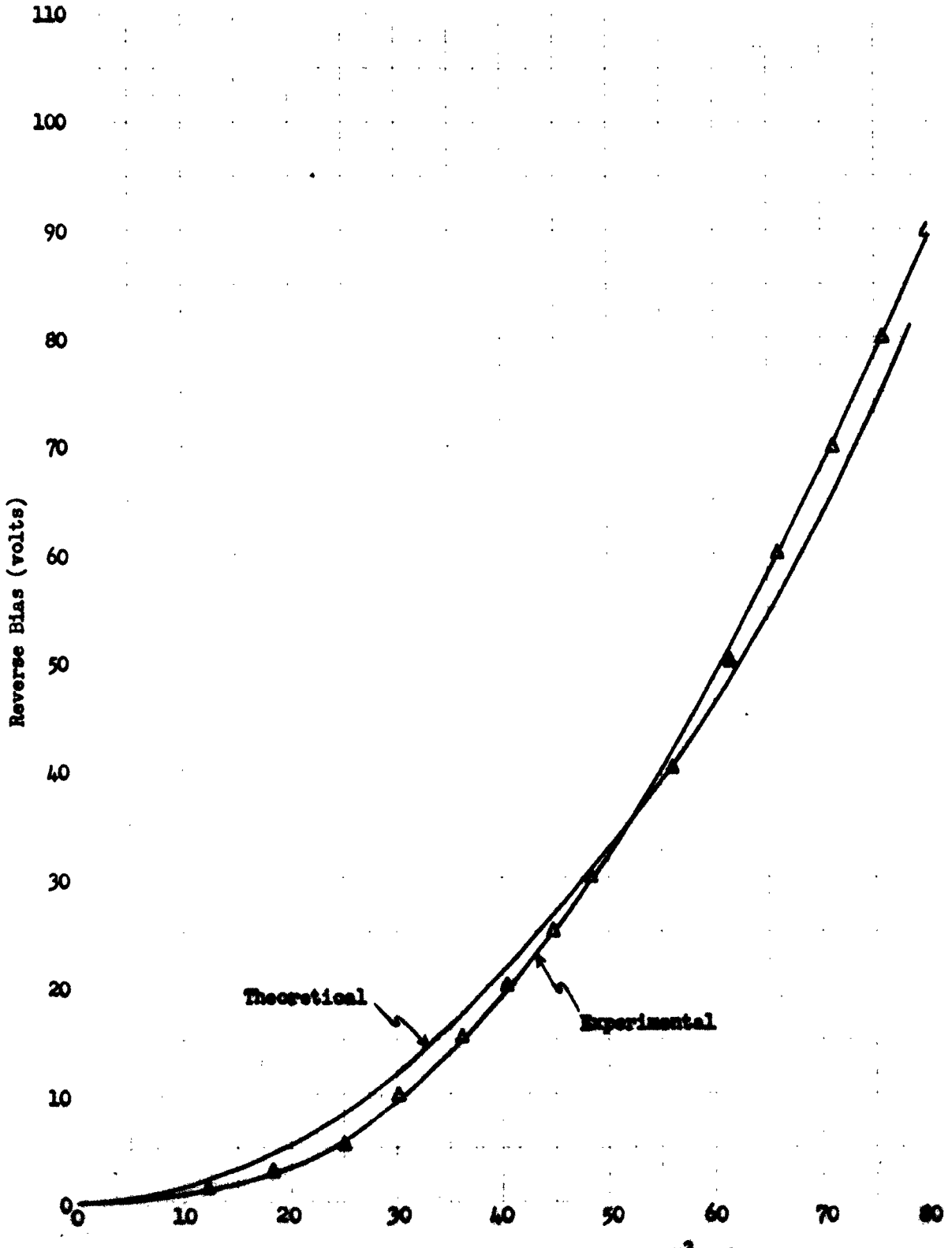

Figure 4. Movement of Depletion Layer on Bevel

B. Cutoff Characteristics

The cutoff characteristics of the ADC can now be considered, since equations for the movement were developed in the preceding section. The current path of the probe does not lend itself to a rigorous mathematical solution, so an empirical approach will be used.

When a probe is positioned on the bevel and connected electrically to the N-side, it can be characterized as a point contact diode. The field through the N-type silicon will be maximum along the surface under the probe and decrease as a function of distance below the probe. This distribution is complicated by the point source appearance of the probe (probe appears as a point source on an infinite sheet of silicon) and the coordinate positions of the point contact with respect to the N-contact. The flow direction of current is not important in this analysis, but the current density distribution below the probe, which interacts with the movement of the depletion region, has an important relationship to cutoff.

Contact to the high resistivity N-type material by various metal probes gave ohmic characteristics. The test of these probes was made on a PN wafer which had its P-side lapped off. The N-type surface was polished and etched in the same manner as the beveled wafer, and the same pressure was applied to the probes as for the beveled case. Figure 5 is a log-log plot of the V-I

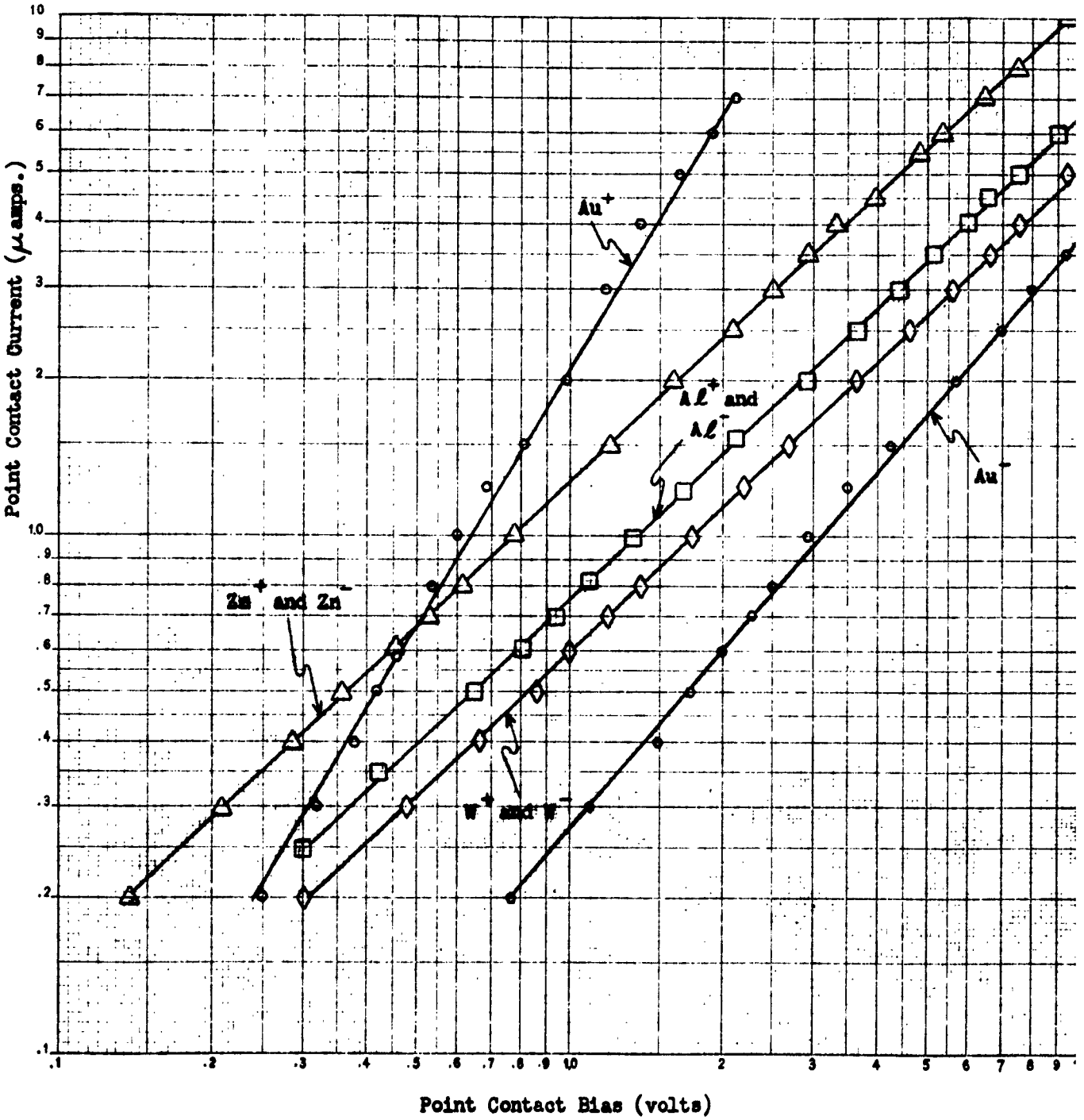

Figure 5. Forward and Reverse Characteristics of Metal Probes

characteristics of various metal pressure contacts to the N-substrate. The forward and reverse V-I characteristics of the tungsten, zinc, and aluminum probes are the same, and the slope in each case is approximately that of an ohmic contact. The magnitude of the current calculated from Ohm's law was within the right order of magnitude and the translation between the three curves can be attributed to the increase in contact area for the various probes The gold probe appears to make rectifying contact to the N-material where the forward current is shown to be greater than the reverse current. This experiment was performed immediately after the wafer was etched and several times within the following few days with no change in any of the characteristics.

The tungsten probe has been used predominantly in testing. The ohmic characteristics of the tungsten probe on the bevel can be shown by plotting the forward and reverse resistances of the contact as a function of distance down the wafer.[18] The resistances are approximately equal.

An experiment was carried out to obtain an empirical equation for the current density distribution below the probe. The tungsten probe was placed at a floating potential of 80 volts, approximately 28 mils up the bevel from the junction. This position is well above the junction, and should not influence the current path. The V-I characteristics of the probe were taken with various

---

(18) 3rd Quarterly Progress Report, Solid State Analog-to-Digital Converter, NOw 62-0749-d, Aerial Measurements Laboratory, Northwestern University, November-December 1962, January 1963.

reverse biases on the PN bevel and are plotted in Figure 6. This technique, in effect, shows the decrease in probe current as the depletion region moves toward the contact reducing the current channel. Since the relationship between the reverse voltage (V_R) of the wafer and the movement of the depletion layer has been previously determined, the various reverse voltages can be related to decreases in the width of the channel below the probe.

Figure 7 is a plot of normalized probe current (at a constant probe voltage) versus the width of the depletion region (along the bevel and in the bulk). This is a plot taken from Figure 6 at a constant voltage where the reverse voltage has been related to movement by Equation (17a) of the last section. The width of the channel below the probe as a function of normalized current density can now be plotted since the position of the probe above the junction is known. Figure 8 is a plot of channel depth versus normalized probe current taken from Figure 7. This curve shows the increase in current with increasing channel width. An exponential can be fitted to this curve where the best fit is:

$$I/I_O = \left[1 - \text{exponential} - (4.25 \times 10)\, X'\right] \qquad (18)$$

where X' is vertical distance below the probe in mils.

Equation (18) can be considered a general equation for the cutoff characteristic by making a transformation of the origin from the

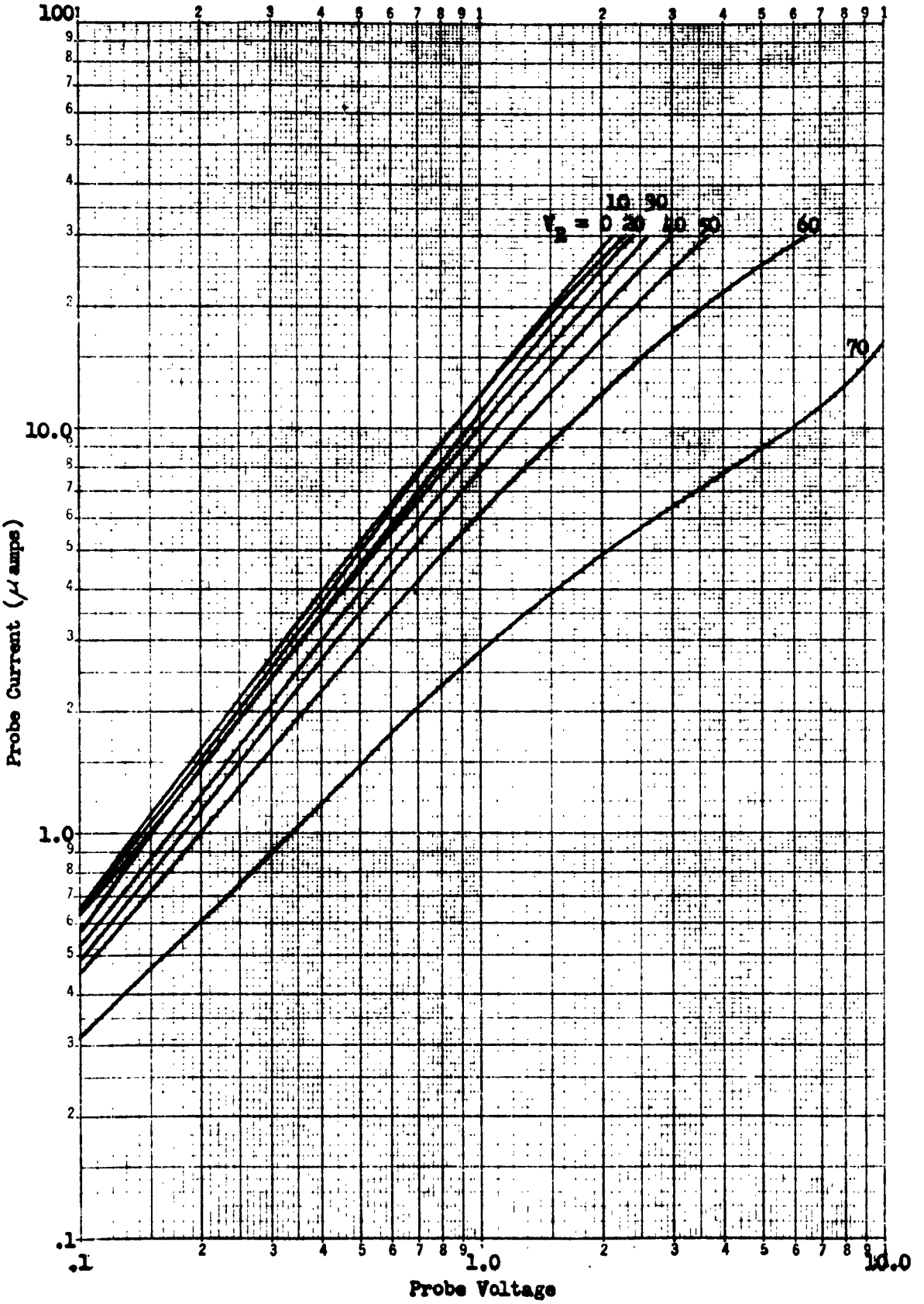

Figure 6. V-I Characteristics of Tungsten Probe on Bevel

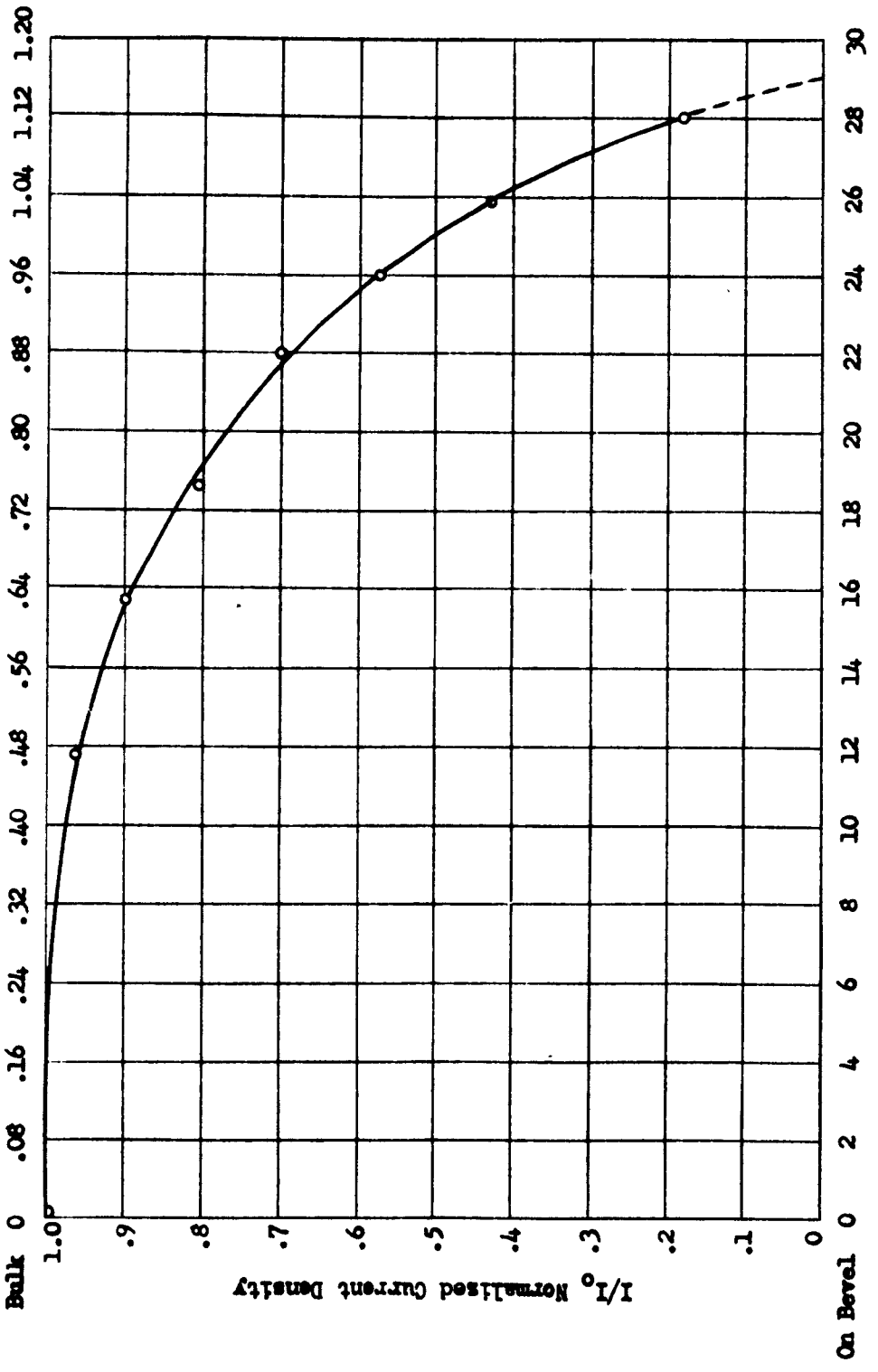

Figure 7. Normalized Probe Current with Increasing Depletion Region

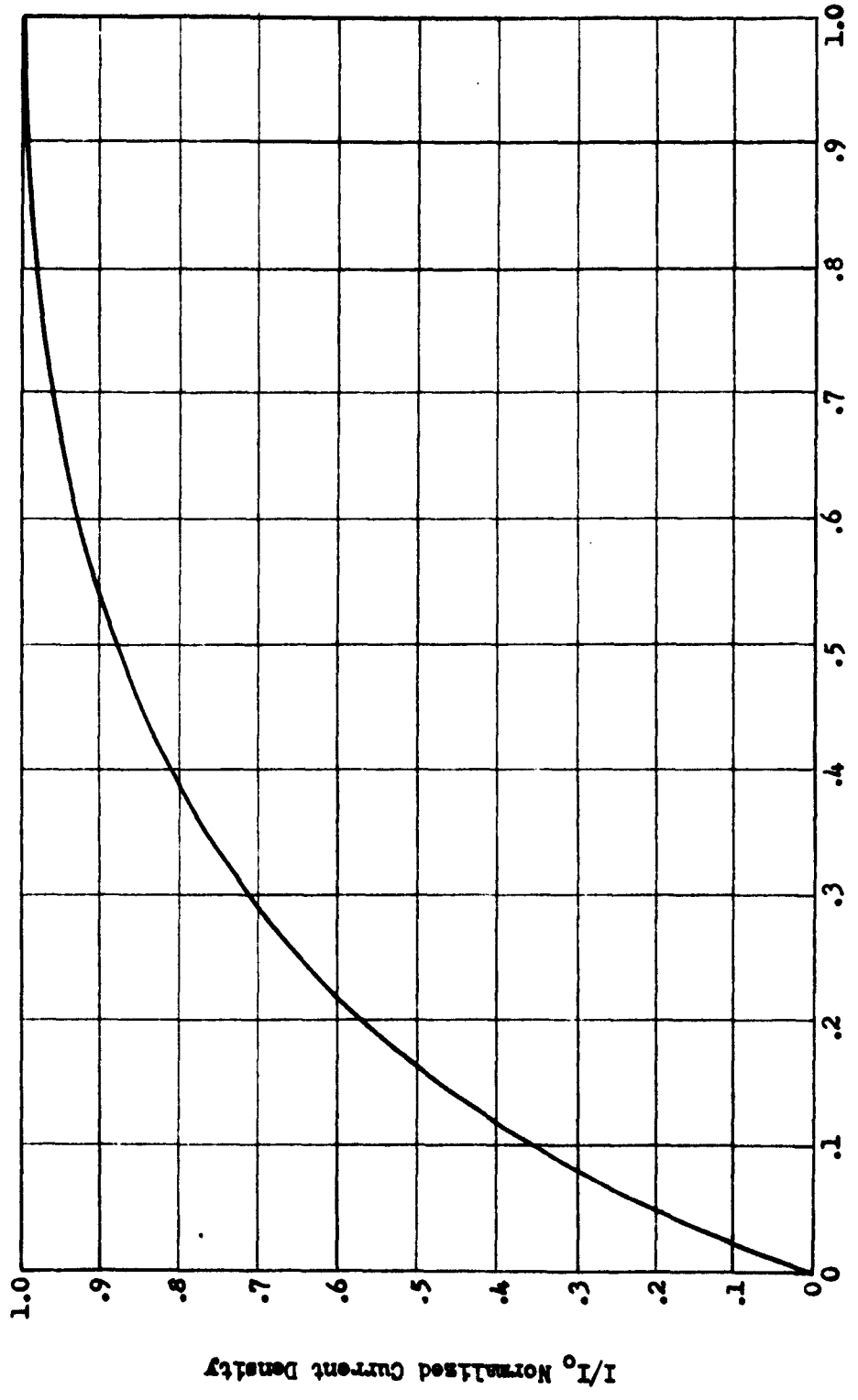

Figure 8. Normalized Probe Current with Increasing Channel Depth

Equation (21) was obtained from empirical results and theoretical calculations. The current I_o must be calculated for $V_R = 0$ at each V_{fo} and the floating potential is given by the open circuit voltage of the particular probe. This equation gives a good fit to the experimental results but only through further test can a best fit be obtained.

Figure 9 shows a series of cutoff characteristics obtained with a single probe positioned at different floating potentials. These curves are typical of a family of curves obtained from multiple probes. There are discrepancies in these characteristics which are not considered in the present derivation but which will be compensated for through more experimental data.

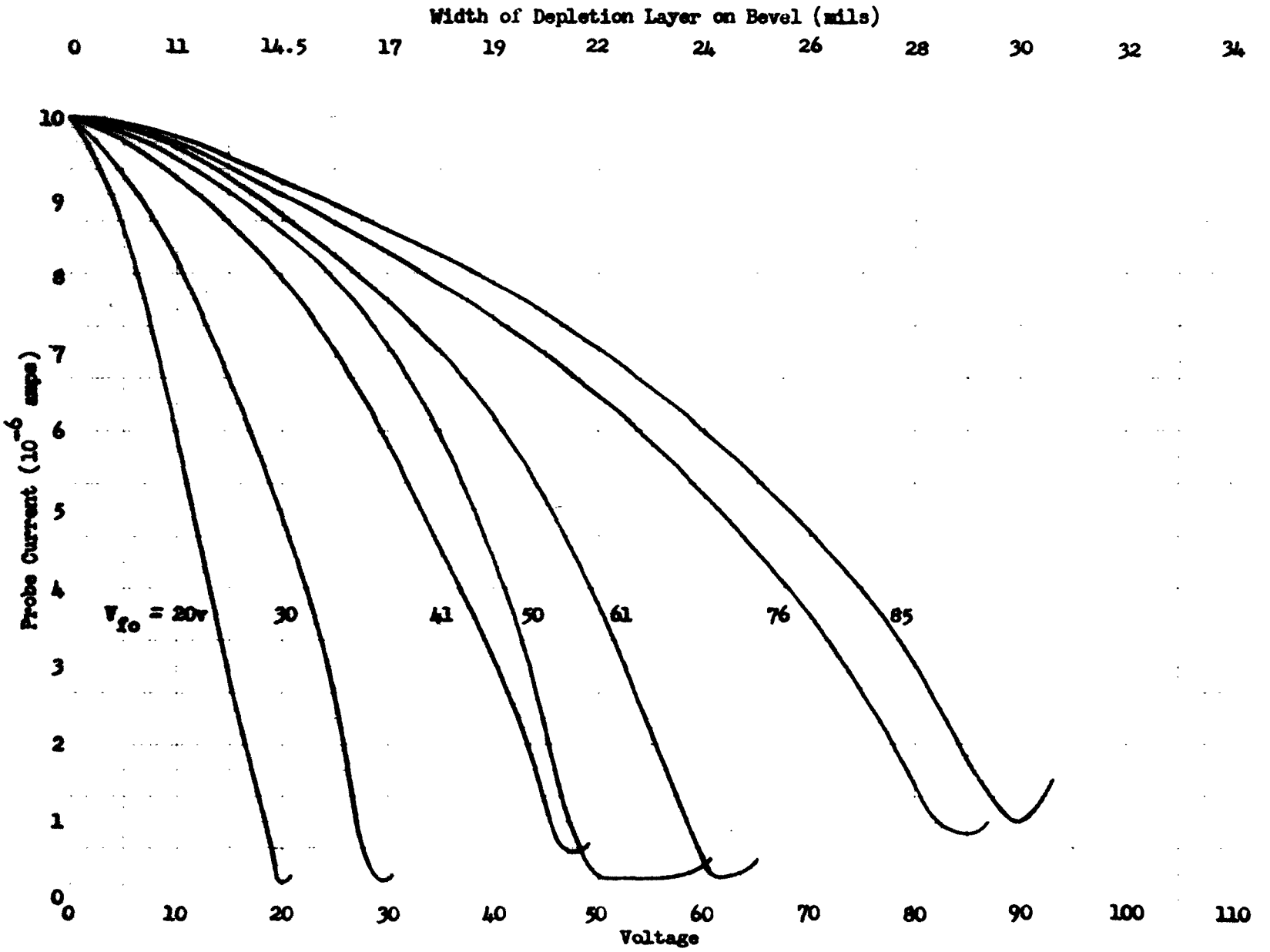

Figure 9. Probe Cutoff Characteristics

IV. Summary and Results

The movement of the depletion region can be described by the abrupt junction solution times the amplification angle for the beveled unit. The resistivity of the N-type silicon is important in this solution and from all indications a more accurate check of resistivity is required. The abrupt junction solution gives a good fit for these wafers but each new diffused junction must be checked as to how well it follows the approximations used.

The cutoff characteristics can be described by the equations given. These equations are empirical because of the nature of the current path and through further studies a better fit can be obtained. These equations will be useful in defining the resolution of the device.

V. Future Work

With the equipment presently being reworked, positioning of multiple probes will be carried out in the dry box. The positioning and attaching of probes to the beveled surface will be attempted again but with more control of the ambient atmosphere and the surface. Electrical characteristics of the multiple probe cutoffs will be taken and compared to the cutoff equation presented in this report.